Coupling the CWRF with the CICE for Arctic Climate Applications

Xin-Zhong Liang, Jianping Pan, Kenneth Kunkel
Illinois State Water Survey, University of Illinois at Urbana-Champaign
Julian X.L. Wang
Air Resources Laboratory, National Oceanic and Atmospheric Administration
Elizabeth C. Hunke and William H. Lipscomb
T-3 Fluid Dynamics Group, Los Alamos National Laboratory

Abstract

The Climate extension of the Weather Research and Forecasting model (CWRF) is being coupled with the Los Alamos Sea Ice Model (CICE) to simulate sea ice and climate variations over the Arctic. This study presents the development of the coupling interfaces and procedures. For the purpose of evaluation and initialization, the CICE is run in a standalone mode over an extended Arctic domain at 50 km grid spacing. The NCEP-DOE AMIP II reanalysis during 1981-1985 are used to drive the CICE. It is shown that the CICE captures the basic spatial distributions and temporal variations of Arctic sea ice cover, except for a general overestimation. The overestimation may result from cold biases in the reanalysis, satellite underestimates, or the lack of surface-atmosphere interactions in the standalone mode. The coupled CWRF-CICE integration will facilitate the study on how the downscaling improves the representation of the regional circulation and surface energy budget, and hence local sea ice and climate changes over the Arctic.

Introduction

The Arctic is a region of critical importance and vulnerability to global climate variability and change (Randall et al. 1998, Serreze et al. 2000, Oechel et al. 2000, IPCC 2001). It involves complicated interactions between atmosphere, land, sea ice, and ocean processes with positive and negative feedbacks that are not fully understood. To better address challenging scientific issues, several regional climate models (RCMs) have been developed for Arctic applications (Walsh et al. 1993, Lynch et al. 1995, Dethloff et al. 1996, Jürrens 1999, Wei et al. 2002). Among these, the Arctic Region Climate System Model (ARCSyM, Lynch et al. 1995, 1997, 1998, 1999) is the *single available fully-coupled* RCM that integrates the hydrostatic MM4-based RegCM2 (Giorgi et al. 1993) for atmosphere, the LSM (Land Surface Model, Bonan 1996) for land, a sea ice model accounting for both thermodynamics (Parkinson and Washington 1979, Schramm et al. 1997) and dynamics (Hunke and Dukowicz 1997), and a primitive-equation ocean model (Mell and Kantha 1989, Kantha and Clayson 1994, Bailey et al. 1997). The ARCSyM has since been widely used in various studies of sea ice (e.g., Wu and Lynch 2000, Maslanik et al. 2000, Rinke et al. 2000, and references therein).

Meanwhile, individual components of the ARCSyM have been substantially improved in both physics representation and supercomputing capability. In particular, the next-generation Weather Research and Forecasting model (WRF) is being developed by a broad community of government and university researchers (Klemp et al. 2000, Michalakes 2000, Chen and Dudhia 2000, http://www.wrf-model.org/). Since the WRF is built upon the most advanced supercomputing technologies and promises greater efficiency in computation and flexibility in new module incorporation, it will eventually supercede the MM5 (an advanced, non-hydrostatic version of the MM4). To extend its capability for applications on regional climate scales, we have developed the CWRF (see Liang et al. 2004 for an introductory description). The CWRF has incorporated the state-of-the-art Common Land Model (CLM, Dai et al. 2003) with numerous crucial updates for land processes, and is currently being coupled with the latest Geophysical Fluid Dynamics Laboratory Modular Ocean Model (MOM, Griffies et al. 2003) and Los Alamos Sea Ice Model (CICE, Hunke and Lipscomb 2002) to predict ocean temperature, salinity, current and sea ice distributions. When fully developed, the coupled system will be an alterative, and most likely an improved one, of the ARCSyM. This study presents the development of the coupling interfaces and procedures between the CWRF and CICE, focusing on preliminary evaluation and initialization, where the CICE is run in a standalone mode.

CWRF and CICE Description

The WRF was originally designed mainly for numerical weather predictions (NWP) and not expressly for climate studies. To extend its capability for applications on regional climate scales, we have developed the CWRF with four crucial characteristics to improve: [1] *planetary-mesoscale interaction* by including an optimal buffer zone treatment that integrates realistic energy and mass fluxes across the lateral boundaries of the RCM domain (Liang et al.

2001); [2] *surface-atmosphere interaction* by incorporating new physics modules for planetary boundary layer, land surface and terrestrial hydrology as well as observed variations or dynamic predictions of vegetation, ocean and sea ice; [3] *convection-cloud-radiation interaction* by implementing fully-coupled, new physical parameterizations for cumulus, cloud microphysics, cloud formation, and radiative transfer; and [4] *system consistency throughout all process modules* by utilizing unified water vapor saturation and solar zenith angle functions, common physical constants and coherent tunable parameters.

The concept of the CWRF is in its emphasis on the “extension” of the WRF. This extension incorporates inclusively all WRF functionalities for NWP while enhancing the capability for climate applications. As such, the CWRF can be applied for both weather forecasts and climate predictions. This unification offers an unprecedented opportunity to develop, test, and verify new physical parameterizations of unresolved processes, identify their systematic errors, and eventually improve them over a wide range of frequencies from weather to climate scales. A series of papers are being prepared to document details of the CWRF formulations and skills in weather forecasts and climate predictions. The first of the series depicts the construction and implementation of surface boundary conditions, where the CWRF concept and its major modules representing surface-atmosphere interactions are briefly described (Liang et al. 2004).

The CICE integrates several interactive components (Hunke and Lipscomb 2004), including an energy-conserving thermodynamic model that computes local growth rates of snow and ice due to vertical conductive, radiative and turbulent fluxes, along with snowfall (Bitz and Lipscomb 1999); an elastic-viscous-plastic model (EVP) of sea-ice dynamics (Hunke and Dukowicz 1997, Hunke and Dukowicz 2002) predicting the ice velocity and deformation rates; an incremental remapping transport scheme describing the advection of the real ice concentration, volume and thermodynamic properties (Lipscomb and Hunke 2004); and a ridging parameterization that transfers ice among five thickness categories based on energetic balances and strain rates (Thorndike et al. 1975).

CWRF and CICE Coupling

To couple with the CWRF, the CICE coding structure has been modified to follow the WRF standard, which adopts a layered software architecture promoting modularity, portability, and software reuse (Michalakes 2000). The architecture consists of three distinct model layers: a solver layer that describes the core of a dynamic or physical representation, a driver layer that is responsible for allocating and deallocating space and controlling the integration sequence and I/O, and a mediation layer that communicates between the driver and model layers. The WRF incorporates a flexible approach for parallelism through a two-level decomposition in which the model domain may be subdivided into patches that are assigned to distributed-memory nodes and then may be further subdivided into tiles that are allocated to shared-memory processors within a node. This approach addresses all current models for parallelism: single processor, shared memory, distributed memory, and hybrid. The WRF has a built-in Registry mechanism, which is invoked at compile time to automatically generate interfaces between the driver and model layers in the software architecture, calls to allocate state fields within the derived data type representing the computational domains, communicators for various halo exchanges used in the different dynamical cores, and calls to the WRF input/output application program interface (I/O API) for initial, restart, and history I/O.

The original CICE source code contains over 30 files, having more than 120 subroutines/functions. All variables are defined with the global dimensional sizes; their I/O uses in individual subroutines/functions and information exchanges between them are not explicitly declared; and the parallel processing is implemented with the MPI message passing called in each subroutine as needed. We have combined all files into a single package that consists of 4 principle modules called in the sequential order: initial, thermodynamic, dynamic (EVP and transport), and ridging. The initial and dynamic modules require specific halo structures for I/O variables depending on adjacent grids, while the other two using only local fields have none. Because the time-steps for the thermodynamic and dynamic modules often differ, the separation facilitates their easier implementation into the WRF mediation layer. All key parameters and predictive or diagnostic variables are defined in the Registry with the global dimensional sizes specified by the domains as well as their respective halo structures if required. Intermediate variables without I/O are declared as local working space with exact array size bounds as needed.

In addition, the original code does not consider the mapping projection factors. For a full, consistent coupling with the CWRF, the mapping factors for various projections are incorporated. For example, the continuity equation is now written as:

$$\frac{\partial \rho}{\partial t} + m^2 \left\{ \frac{\partial}{\partial x}\left(\frac{\rho u}{m}\right) + \frac{\partial}{\partial y}\left(\frac{\rho v}{m}\right) \right\} + \frac{\partial}{\partial z}(\rho w) = 0$$

where ρ is ice concentration, (u, v, w) ocean current, and m the map scale factor from the CWRF.

Domain and Experiment Design

The testing domain is designed to include the Arctic region that has available data measured by the Scanning Multichannel Microwave Radiometer (SSMR) on board the Nimbus-7 satellite (http://geochange.er.usgs.gov/pub/sea_ice/). It has 168×235 grids at 50 km spacing, using a polar stereographic map projection centered at 90°N, 45°W. The domain covers an extended area where most of the Arctic sea ice presents.

The CICE simulation starts from rest, where ice cover and thickness are prescribed depending on the initial input of sea surface temperature and salinity distributions. Monthly mean sea surface temperature, salinity (Steele and Ermold 2001), and current (Mariano et. al. 1995) data are available at a global 1° longitude-latitude grid mesh. They are specified as initial or surface boundary conditions, linearly interpolated in time during the entire integration. The NCEP-DOE AMIP II reanalysis (R-2, Kanamitsu et al. 2002) during 1981-1985 at 2.5° grid spacing and a 6-hourly interval are used to drive the CICE. All data were linearly mapped onto the CWRF grid. In this standalone simulation, ice-free is assumed in the lateral buffer zones. To achieve a quasi-equilibrium in initialization, the CICE integration driven by the 1981 time-varying conditions is repeated (i.e., cycling throughout the year) for 5 years. After this perpetual run, a full integration begins where the driving conditions vary as observed during 1981-1985. The integration is repeated for a 2nd cycle, whose result shows small differences from the 1st cycle, indicating that a quasi-equilibrium state has been reached.

Results and Discussion

The Arctic sea ice cover reaches a maximum in March and a minimum in September. Figure 1 compares 1981-1985 averaged March and September mean sea ice cover distributions between SSMR measurements and CICE simulations. In general, the CICE captures well the ice formation and melting processes during the year. The model seems to overestimate the rates for both processes, producing more extensive ice over in September and less in March. On an annual average, the CICE has sea ice cover over 11.64×10^6 km^2, which is more than the SSMR value of 8.97×10^6 km^2. On the other hand, the in situ data (see Fig. 2.15 of IPCC 2001) shows an ice extent of approximately 12×10^6 km^2. We are not certain what is the ground truth since the extent, assuming binary ice cover, does not consider leads (the presence of open water within an ice pack), causing an overestimation, while SSMR may also be biased to underestimation as derived from the SSM/I algorithm, especially during melting seasons (Steffen et al. 1992).

Several additional uncertainties may attribute to the CICE and SSMR differences. First, the R-2 uses a coarse resolution, where sea ice is defined as binary. The driving meteorological conditions based on the R-2 may likely contain cold biased in winter, leading to more ice cover in the model. Sensitivity experiments with different reanalyses as the driving conditions and comparisons with the POLES surface air temperature data (Martin and Munoz 1997) are in progress to determine the existence of R-2 cold biases and its impact. Second, the sea surface temperature, salinity, and current distributions are long-term climatological means at a coarse resolution, and may not represent the real conditions during 1981-1985, especially over the sea ice margins. Given that the CICE predicts sea surface temperature variations in a mixed-layer ocean as a result of the energy balance driven by the R-2 reanalysis, the sea surface temperature input may not be important. We anticipate that the sea surface current is a sensitive driving factor, the uncertainty of which is large. Third, in the standalone mode, the lack of surface-atmosphere interactions may cause the CICE to overestimate the sea ice formation, as we have experienced in global model simulations. All these issues will be more thoroughly studied by applying the CWRF that fully coupled with the CICE and MOM.

Acknowledgement. We thank the NCAR/MMM for the WRF modeling systems, and NCSA/UIUC and NOAA/FSL for supercomputing support. The research was partially supported by the National Science Foundation grant EAR0209009 and the NOAA/HU NCAS grant 634554172523.

References

Bailey, D.A., A.H. Lynch, and K.S. Hedström, 1997: The impact of ocean circulation on regional polar simulations using the Arctic regional climate system model. *Ann. Glaciol*., **25,** 203-207.

Bitz, C.M., and W.H. Lipscomb, 1999: An energy-conserving thermodynamic model of sea ice. *J. Geophys. Res*., **104,** 15669-16677.

Bonan, G.B., 1996: *A Land Surface Model (LSM version 1.0) for Ecological Hydrological, and Atmospheric Studies: Technical Description and User's Guide*., NCAR Tech. Note, NCAR/TN-417+STR, National Center for Atmospheric Research, Boulder, CO, 150 pp.

Chen, S.-H., and J. Dudhia, 2000: *Annual Report: WRF Physics.* (http://www.mmm.ucar.edu/wrf/users/wrf-doc-physics.pdf).

Christensen, J.H., and P. Kuhry, 2000: High resolution regional climate model validation and permafrost simulation for the East-European

Russian Arctic. *J. Geophys. Res.*, **105**, 29647-29658.

Dai, Y., X. Zeng, R.E. Dickinson, I. Baker, G.B. Bonan, M.G. Bosilovich, A.S. Denning, P.A. Dirmeyer, P.R. Houser, G. Niu, K.W. Oleson, C.A. Schlosser, and Z-L. Yang, 2003: The Common Land Model. *Bull. Amer. Meteor. Soc*., **84**, 1013-1023.

Dethloff, K., A. Rinke, R. Lehmann, J.H. Christenen, M. Botzet, and B. Machenhauer, 1996: A regional climate model of the Arctic atmosphere. *J. Geophys. Res.*, **101,** 23401–23422.

Giorgi, F., M.R. Marinucci, and G.T. Bates, 1993: Development of a second-generation regional climate model (RegCM2). Part I: Boundary layer and radiative transfer processes. *Mon. Wea. Rev.*, **121**, 2794-2813.

Griffies, S.M., M.J. Harrison, R.C. Pacanowski, and A. Rosati, 2003: *A Technical Guide to MOM4*. GFDL Ocean Group Technical Report No. 5, NOAA/Geophysical Fluid Dynamics Laboratory, 337 pp. (http://www.gfdl.noaa.gov/~fms/).

Hunke, E.C., and J.K. Dukowicz, 1997: An elastic-viscous-plastic model for sea ice dynamics. *J. Phys. Oceanogr*., **27,** 1849-1867.

Hunke, E.C., and J.K. Dukowicz, 2002: The elastic-viscous-plastic sea ice dynamics model in general orthogonal curvilinear coordinates on a sphere-effect of metric terms. *Mon. Wea. Rev.*, **130**, 1848-1865.

Hunke, E.C., and W.H. Lipscomb, 2004: *CICE: The Los Alamos Sea Ice Model Documentation and Software User's Manual*, T-3 Fluid Dynamics Group, Los Alamos National Laboratory.

IPCC, 2001: *Climate Change: The Scientific Basis.* Contributions of Working Group 1 to the Third Assessment Report of the Intergovernmental Panel on Climate Change. J.T. Houghton, Y. Ding, D.J. Griggs, M. Noguer, P.J. van der Linden, X. Dai, K. Maskell, and C.A. Johnson (Eds.),Cambridge University Press, Cambridge and New York, 881 pp.

Jürrens, R., 1999: Validation of surface fluxes in climate simulations of the Arctic with the regional model REMO. *Tellus*, **51A,** 698–709.

Kanamitsu, M., W. Ebisuzaki, J. Woollen, S.-K. Yang, J.J. Hnilo, M. Fiorino, and G.L. Potter, 2002: The NCEP-DOE AMIP-II reanalysis (R-2). *Bull. Amer. Meteor. Soc.*, **83**, 1631-1643.

Kantha, L.H., and C.A. Clayson, 1994: An improved mixed layer model for geophysical applications. *J. Geophys. Res.*, **99**, 25235-25266.

Klemp, J., W. Skamarock, and J. Dudhia, 2000: Conservative split-explicit time integration methods for the compressible nonhydrostatic equations: WRF Eulerian prototype model equations on height and mass coordinates. (http://www.mmm.ucar.edu/wrf/users/wrf-dyn-num.html).

Liang, X.-Z., H. Choi, K.E. Kunkel, Y. Dai, E. Joseph, J.X.L. Wang, and P. Kumar, 2004: Development of the regional climate-weather research and forecasting model (CWRF). Part A: Surface boundary conditions. *J. Climate* (submitted).

Liang, X.-Z., K.E. Kunkel, and A.N. Samel, 2001: Development of a regional climate model for U.S. Midwest applications. Part 1: Sensitivity to buffer zone treatment. *J. Climate*, **14**, 4363-4378.

Lipscomb, W.H., and E.C. Hunke, 2004: Modeling sea ice transport using incremental remapping. *Mon. Wea. Rev.* (in press)

Lynch, A.H., G.B. Bonan, F.S. Chapin III, and W. Wu, 1999: The impact of tundra ecosystems on the surface energy budget and climate of Alaska. *J. Geophys. Res.*, **104**, 6647–6660.

Lynch, A.H., W.L. Chapman, J.E. Walsh, and G. Weller, 1995: Development of a regional climate model of the western Arctic. *J. Climate*, **8**, 1555–1570.

Lynch, A.H., D.L. McGinnis, W.L. Chapman, and J.S. Tilley, 1997: A Multivariate comparison of two land surface models integrated into an Arctic regional climate system model. *Ann. Glaciol*., **25**, 127-131.

Lynch, A.H., D.L. McGinnis, and D.A. Bailey, 1998: Snow-albedo feedback and the spring transition in a regional climate system model: Influence of land surface model. *J. Geophys. Res*., **103**, 29037-29049.

Martin, S.E., and E. Munoz, 1997: Properties of the Arctic 2-m air temperature for 1979-1993 derived from a new gridded dataset. *J. Climate*, **10**, 1420-1440.

Mariano, A.J., E.H. Ryan, B.D. Perkins, and S. Smithers, 1995: The Mariano global surface velocity analysis 1.0. *U.S. Coast Guard Technical Report*, CG-D-34-95.

Maslanik, J.A., A.H. Lynch, and M. Serreze, 2000: A case study simulation of Arctic regional climate in a coupled model. *J. Climate*, **13**, 383-401.

Mellor, G., and L. Kantha, 1989: An ice-ocean coupled model. *J. Geophys. Res.*, **94**, 10937-10954.

Michalakes, J., 2000: Weather research and forecast model 1.0: Software design and implementation. (http://www.mmm.ucar.edu/wrf/users/wrf-architect.html).

Oechel, W.C., G.L. Vourlitis, S.J. Hastings, R.C. Zulueta, L. Hinzman, and D. Kane, 2000: Acclimation of ecosystem CO2 exchange in the Alaskan Arctic in response to decadal climate warming. *Nature*, **406,** 978–981.

Parkinson, C.L., and W.M. Washington, 1979: A large scale numerical model of sea ice. *J. Geophys. Res.*, **84**, 311-337.

Randall, D., J**.** Curry, D. Battisti, G. Flato, R. Grumbine, S. Hakkinen, D. Martinson, R. Preller, J. Walsh, and J. Weatherly, 1998: Status of and outlook for large-scale modeling of atmosphere-ice-ocean interactions in the Arctic*. Bull. Am. Met. Soc.*, **79**, 197-219.

Rinke, A., and K. Dethloff, 1999: Sensitivity studies concerning initial and boundary conditions in a regional climate model of the Arctic. *Clim. Res*., **14**, 101-113.

Rinke, A., A.H. Lynch, and K. Dethloff, 2000: Intercomparison of Arctic regional climate simulations: Case studies of January and June 1990. *J. Geophys. Res.*, **105**, 29669-29683.

Schramm, J.L., M.M. Holland, J.A. Curry; E.E. Ebert, 1997: Modeling the thermodynamics of a sea ice thickness distribution, 1, Sensitivity to ice thickness resolution. *J. Geophys. Res.,* **102**, 23079-23091.

Serreze, M.C., J.E. Walsh, F.S. Chapin III, T. Osterkamp, M. Dyurgerov, V. Romanovsky, W.C. Oechel, J. Morison, T. Zhang, and R.G. Barry., 2000: Observational evidence of recent change in the northern high-latitude environment. *Climatic Change*, **46**, 159-207.

Steele, M., R. Morley, and W. Ermold, 2001: A global ocean hydrography with a high quality Arctic Ocean. *J. Climate*, **14**, 2079-2087. (http://dss.ucar.edu/datasets/ds285.2/data/)

Steffen, K., D.J. Cavalieri, J.C. Comiso, K.St. Germain, P. Gloersen, J. Key, and U. Rubinstein, 1992: The estimation of geophysical parameters using passive microwave algorithms. *Microwave Resmote Sensing of Sea Ice, Geophys. Monogr*., **68**, F. Carsey (Ed.), Amer. Geophys. Union, 243-259.

Thorndike, A. S., D.A. Rothrock, G.A. Maykut, and R. Colony, 1975: The thickness distribution of sea ice. *J. Geophys. Res*., **80,** 4501-4513.

Walsh, J.E., A. Lynch, and W. Chapman, 1993: A regional model for studies of atmosphere-ice-ocean interaction in the western Arctic. *Meteor. Atmos. Phys.*, **51,** 179-194.

Wei, H., W.J. Gutowski Jr., C.J. Vorosmarty, and B.M. Fekete, 2002: Calibration and validation of a regional climate model for Pan-Arctic hydrologic simulation. *J. Climate*, **15**, 3222-3236.

Wu, W., and A.H. Lynch, 2000: Response of the seasonal carbon cycle in high latitudes to climate anomalies. *J. Geophys. Res.,* **105,** 22897-22908.

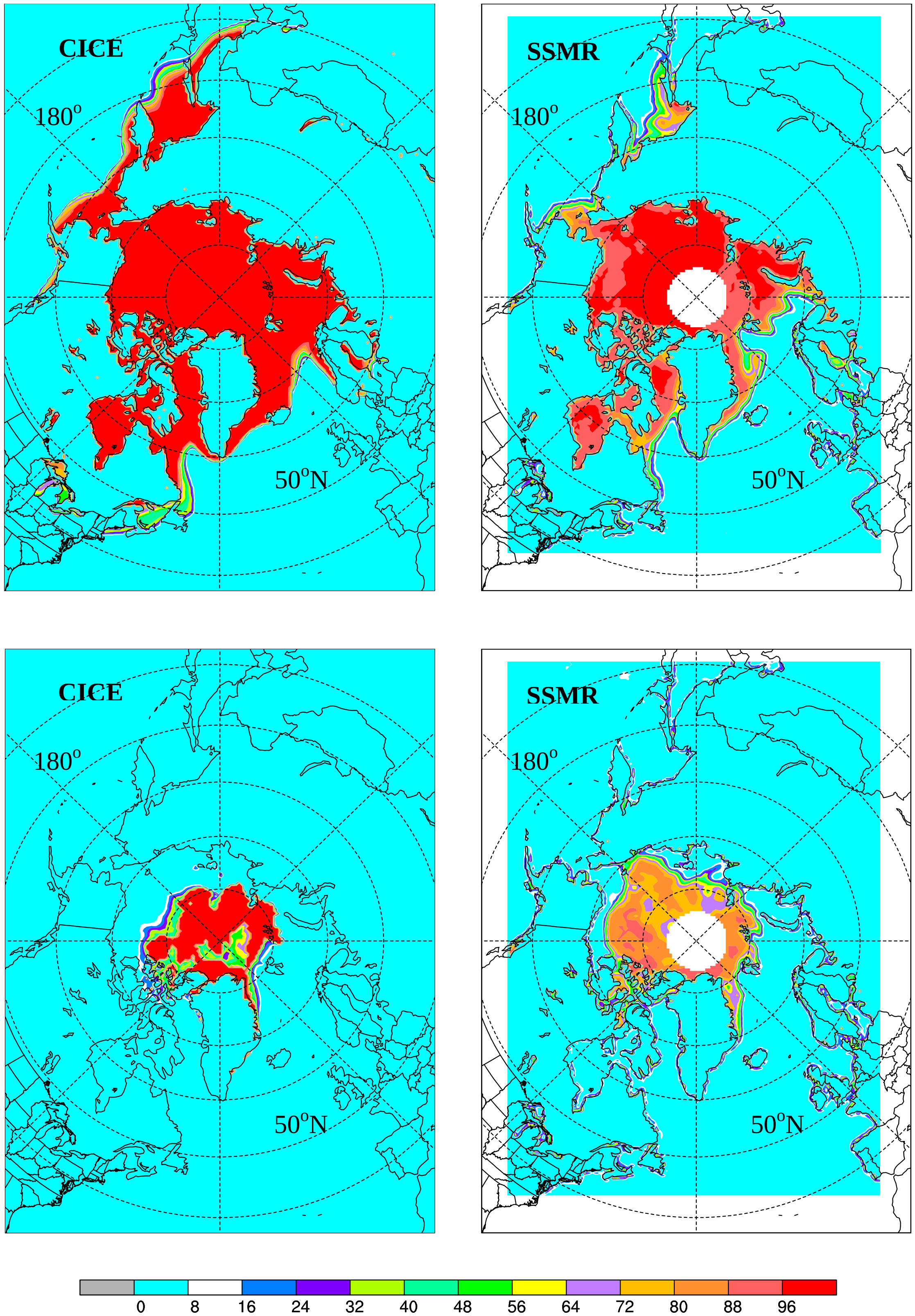

Figure 1. Sea ice area cover (%) simulated by CICE (*left*) and observed by SSMR (*right*) in March (*top*) and September (*bottom*) averaged during 1981-1985.